Parvinder Singh and Atul Kumar*

# Correlations, Nonlocality and Usefulness of an Efficient Class of Two-Qubit Mixed Entangled States

https://doi.org/10.1515/zna-2017-0322
Received September 14, 2017; accepted January 9, 2018

**Abstract:** We establish an analytical relation between the Bell-Clauser-Horne-Shimony-Holt (Bell-CHSH) inequality and weak measurement strengths under noisy conditions. We show that the analytical results obtained in this article are of utmost importance for proposing a new class of two-qubit mixed states for quantum information processing. Our analysis further shows that the states proposed here are better resources for quantum information in comparison to other two-qubit mixed entangled states.

**Keywords:** Bell Inequality; Communication Protocols; Entanglement; Quantum Correlations.

## 1 Introduction

The use of entangled resources for efficient communication in comparison to their classical counterparts is based on the existence of long-range correlations between entangled qubits [1–5]. Such correlations not only distinguish between the quantum and classical world but also provide physical insights into the fundamentals of the quantum theory and the applications of information processing [6–11]. In general, for a bipartite system, the distinction between quantum and classical resources is laid down in terms of Bell-type inequalities whose violation confirms the existence of quantum correlations in the system [12, 13]. The Bell-type inequalities, however, do not account for all nonclassical properties of entangled qubits in mixed states. For example, one can find a mixed bipartite state, which may be entangled but would still not violate the Bell-type inequality. The characterisation and usefulness of such systems for quantum communication and information processing would certainly help us to have a better insight into the nature of quantum correlations. Moreover, recent studies in quantum information have shown that the relationship between nonclassicality and correlations is not limited to entangled systems only but can also be extended to some separable systems [14–18]. The degradation of entanglement and quantum correlation under real experimental setups leads to further questions regarding the usefulness of final resources due to interactions with the environment [19, 20]. In general, the finally shared state will always be a mixed state. Hence, besides the fundamental quest to understand the nature of quantum correlations, it is also important to analyse and characterise the nonlocal properties of the finally shared mixed state so that one can take informed decisions as to whether it is useful or not to use the finally shared state for quantum information processing. Fortunately, entanglement can be protected against noise by performing weak measurements [21–23]. The role of correlations in quantum information and communication, therefore, still requires a much deeper analysis to understand the significance of quantum correlations in security, communication and information processing.

In this article, we revisit the question of analysing the usefulness of quantum correlations under noisy conditions and weak measurements. For this, we derive an analytical relation between the CHSH inequality, noise parameters and strength of weak measurements. Our results show some interesting observations regarding applications of weak measurement and its reversal operations under amplitude damping, phase damping and depolarising noise. The analysis further allows us to propose a class of two-qubit mixed entangled states, which do not violate the Bell inequality for weak measurement strength less than 1/2 but is still useful in quantum information processing. Our analysis shows that these states, although not violating the Bell inequality, are still entangled and have non-zero discord [15, 17]. We further investigate the usefulness of such a class for quantum information processing in terms of teleportation fidelity [24, 25], witness operators [26, 27] and channel capacity for superdence coding protocol [28]. The analysis shows that our states can, indeed, be used for successful information

***Corresponding author: Atul Kumar,** Indian Institute of Technology Jodhpur, Rajasthan-342011, India, E-mail: atulk@iitj.ac.in
**Parvinder Singh:** Indian Institute of Technology Jodhpur, Rajasthan-342011, India, E-mail: PG201283005@iitj.ac.in

processing protocols for certain ranges of noise and weak measurement strength. Interestingly, we found that the states proposed here can be characterised as efficient and useful resources for quantum information processing protocols in comparison to a large set of randomly sampled bi-partite mixed and pure states.

## 2 Nonlocality, Noise and Weak Measurement

The violation of the Bell-CHSH inequality revealed the fundamentally different nature of the quantum theory in comparison to local hidden variable theories. In the generalised case, if Alice and Bob choose their measurements as $A$ or $A'$ and $B$ or $B'$ with equal probability of 1/2, then, the Bell CHSH inequality can be represented as

$$|E(AB)+E(AB')+E(A'B)-E(A'B')|\leq 2 \tag{1}$$

such that $A=\sigma_1\cdot\hat{a}$, and $A'=\sigma_1\cdot\hat{a}'$, where $\hat{a}$, $\hat{a}'$ are unit vectors, and $\sigma_i'$s are spin projection operators. The measurement operators $B$ and $B'$ can be defined in a similar fashion. In general, states violating the Bell-CHSH inequality are considered to be useful resources in quantum information and computation. However, the presence of noise hinders the efficiency of such systems due to degradation of the correlation between the qubits. In order to protect entanglement and quantum correlations from decoherence, several models such as entanglement distillation [29–31], decoherence-free subspace [32, 33], quantum error-correcting codes [34–37] and quantum Zeno effect [38, 39] have been proposed and studied. Recently, a new scheme is developed to protect entanglement from decoherence known as weak measurements and its reversal [21, 40–44]. The concept is fundamental to quantum mechanics and is defined in terms of partial collapse measurement operators associated with positive operator valued measure. The process of weak measurement and its reversal has been found to be very useful to propose interaction-free measurements [45] and to suppress decoherence in single and two-qubit systems [21, 40–44, 46–51]. Moreover, weak measurements have been experimentally implemented in many quantum systems [22, 23, 40, 41, 52–54].

The fundamental theory behind the working principle of weak measurement and its reversal lies in the factual possibility of reversing any partial collapse measurement. The basic approach is to perform weak measurement operations on the individual qubits comprising the quantum system so that the initial state suffers less from the applied noise. After weak measurement, and letting the state pass through a decoherence channel, one performs nonunitary reversal weak measurement operations on the individual qubits to recover the quantum correlations. The optimal strength of the weak measurement reversal operation, corresponding to the initial strength of the weak measurement operation, can be obtained by maximising the entanglement and correlations between the qubits. In the following sub-sections, we analyse the effect of different noise channels and weak measurements on the correlations existing between the qubits of a bipartite state.

### 2.1 Amplitude-Damping Channel

We first proceed to analyse the effect of decoherence and weak measurements by establishing a relation between the maximum expectation value of the Bell-CHSH operator, noise parameter and weak measurement strengths. For this, we start with a scenario where Charlie prepares a two-qubit pure state $|\Psi\rangle=\alpha|00\rangle+\beta|11\rangle$ ($|\alpha|^2+|\beta|^2=1$) and sends one qubit each to Alice and Bob through an amplitude-damping channel. The single-qubit Kraus operators for an amplitude-damping channel can be given as

$$E_0^i=\begin{pmatrix}1 & 0\\ 0 & \sqrt{1-\gamma_i}\end{pmatrix},\ E_1^i=\begin{pmatrix}0 & \sqrt{\gamma_i}\\ 0 & 0\end{pmatrix} \tag{2}$$

where $\gamma$ is the magnitude of decoherence, and $i=1$ or $i=2$ represents the qubit index. Therefore, the two-qubit pure state, after passing through the amplitude-damping channel, evolves as

$$\rho_A^{\gamma}=\sum_{k,l\in(0,1)}(E_k^1\otimes E_l^2)\rho(E_k^{\dagger 1}\otimes E_l^{\dagger 2})=\begin{pmatrix}|\alpha|^2+\gamma_1\gamma_2|\beta|^2 & 0 & 0 & \sqrt{\gamma_1'\gamma_2'}\alpha^*\beta\\ 0 & \gamma_1\gamma_2'|\beta|^2 & 0 & 0\\ 0 & 0 & \gamma_2\gamma_1'|\beta|^2 & 0\\ \sqrt{\gamma_1'\gamma_2'}\alpha\beta^* & 0 & 0 & \gamma_1'\gamma_2|\beta|^2\end{pmatrix} \tag{3}$$

where $\gamma_i'=1-\gamma_i$. In order to find whether the above state violates the Bell-CHSH inequality or not, we need to evaluate the maximum expectation value of the Bell-CHSH operator given in (1). In terms of expectation values, (1) can be re-expressed as

$$B(\rho_A^{\gamma})=\langle\sigma_1\cdot\hat{a}\sigma_2\cdot\hat{b}\rangle+\langle\sigma_1\cdot\hat{a}\sigma_2\cdot\hat{b}'\rangle+\langle\sigma_1\cdot\hat{a}'\sigma_2\cdot\hat{b}\rangle-\langle\sigma_1\cdot\hat{a}'\sigma_2\cdot\hat{b}'\rangle \tag{4}$$

Considering a pair of mutually orthogonal unit vectors $\hat{c}$, $\hat{c}'$ such that $\hat{b}+\hat{b}'=2\cos\theta\hat{c}$, and $\hat{b}-\hat{b}'=2\sin\theta\hat{c}'$, (4) can be rewritten as

$$B(\rho_A^{\gamma})=2[\langle\sigma_1\cdot\hat{a}\sigma_2\cdot\hat{c}\rangle\cos\theta+\langle\sigma_1\cdot\hat{a}'\sigma_2\cdot\hat{c}'\rangle\sin\theta] \quad (5)$$

where unit vectors $a$ and $c$ are defined as

$$\begin{aligned} a&=(\sin\theta_a\cos\phi_a,\ \sin\theta_a\sin\phi_a,\ \cos\theta_a)\\ c&=(\sin\theta_c\cos\phi_c,\ \sin\theta_c\sin\phi_c,\ \cos\theta_c) \end{aligned} \quad (6)$$

Similar definitions stand for $a'$ and $c'$ with prime on angles. The first term representing the expectation value $\langle AC\rangle$ gives

$$\begin{aligned} \langle\sigma_1\cdot\hat{a}\sigma_2\cdot\hat{c}\rangle=(\alpha^2+(2\gamma_1-1)(2\gamma_2-1)\beta^2)\cos\theta_a\cos\theta_c\\ +2\alpha\beta\sqrt{1-\gamma_1}\sqrt{1-\gamma_2}\sin\theta_a\sin\theta_c\cos\phi_{ac} \end{aligned} \quad (7)$$

The expectation value of $\langle AC\rangle$ can be maximised with respect to $\theta_a$, such that

$$\begin{aligned} [\langle\sigma_1\cdot\hat{a}\sigma_2\cdot\hat{c}\rangle]_{\max}=[(\alpha^2+(2\gamma_1-1)(2\gamma_2-1)\beta^2)^2\cos^2\theta_c\\ +4\alpha^2\beta^2(1-\gamma_1)(1-\gamma_2)\sin^2\theta_c]^{\frac{1}{2}} \end{aligned} \quad (8)$$

where we have used the fact that the maximum value of $p\sin\theta_1+q\cos\theta_1$ is $\sqrt{p^2+q^2}$ and $\cos^2\phi_{ac}=\cos^2(\phi_a+\phi_c)=1$. Similarly, the second term representing the expectation value $\langle A'C'\rangle$ gives

$$\begin{aligned} [\langle\sigma_1\cdot\hat{a}'\sigma_2\cdot\hat{c}'\rangle]_{\max}=[(\alpha^2+(2\gamma_1-1)(2\gamma_2-1)\beta^2)^2\cos^2\theta_{c'}\\ +4\alpha^2\beta^2(1-\gamma_1)(1-\gamma_2)\sin^2\theta_{c'}]^{\frac{1}{2}} \end{aligned} \quad (9)$$

Equation (5) is maximized with respect to $\theta$, and therefore, we have

$$\begin{aligned} B(\rho^{\gamma})_{\max}=2[(\alpha^2+(2\gamma_1-1)(2\gamma_2-1)\beta^2)^2(\cos^2\theta_c+\cos^2\theta_{c'})\\ +4\alpha^2\beta^2(1-\gamma_1)(1-\gamma_2)(\sin^2\theta_c+\sin^2\theta_{c'})]^{\frac{1}{2}} \end{aligned} \quad (10)$$

To optimize the expectation value for the operator $B(\rho_A^{\gamma})$, we use the orthogonality relation between $\hat{c}$ and $\hat{c}'$ such as $\cos^2\theta_c=\sin^2\theta_{c'}$, and hence,

$$\begin{aligned} B(\rho_A^{\gamma})_{\text{opt}}=2[(\alpha^2+(2\gamma_1-1)(2\gamma_2-1)\beta^2)^2\\ +4\alpha^2\beta^2(1-\gamma_1)(1-\gamma_2)]^{\frac{1}{2}} \end{aligned} \quad (11)$$

If Charlie sends both the qubits through perfect channels such that $\gamma_i=0$, then, the optimised expectation value of the Bell-CHSH operator will be $2[1+4\alpha^2\beta^2]^{\frac{1}{2}}$ as it should be for transmission through an ideal quantum channel [55].

Figure 1 clearly demonstrates that the Bell-CHSH inequality is violated for a small region only where the value of noise parameters $\gamma_i$ are very small; even for the violation region where the values of noise parameters are small, the violation decreases very fast. The analytical result obtained, here, is in complete agreement with the numerical optimisation of the Bell-CHSH operator for $\rho_A^{\gamma}$. The effect of noise on nonlocality is depicted in Figure 2, which describes the degradation of nonlocal correlations due to decoherence for different initial states, i.e. for different $\alpha$ values. If we consider the noise parameters to be the same, then, the Bell-CHSH inequality is violated by the finally shared states iff $(\alpha^2+\beta^2(1-2\gamma)^2)^2+4\alpha^2\beta^2(\gamma-1)^2>1$. For example, if we start with a maximally entangled

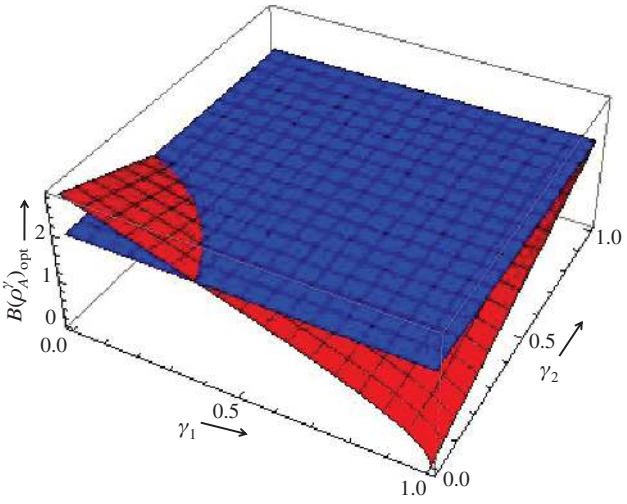


**Figure 1:** Estimation of $B(\rho_A^{\gamma})_{\text{opt}}$ with respect to decoherence parameters $\gamma_1$ and $\gamma_2$ for a maximally entangled two-qubit state.

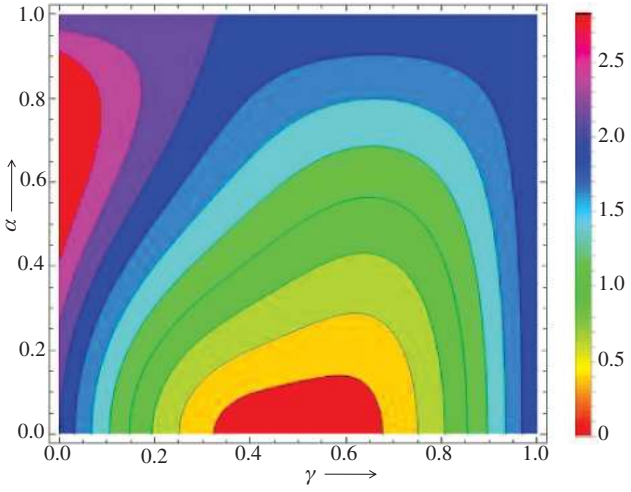


**Figure 2:** Effect of noise parameter $\gamma$, considering ($\gamma_1=\gamma_2=\gamma$) on $B(\rho_A^{\gamma})_{\text{opt}}$ for different two-qubit entangled states.

initial state, then, the range of decoherence parameter for the Bell inequality violation is $0 \le \gamma < 0.2334$. Therefore, if we start with a maximally entangled state, then, the finally shared state does not violate the Bell inequality for $0.2334 \le \gamma \le 1$. Interestingly, the nonviolation region for a state with $\alpha = 0.95$ is $0.3203 \le \gamma \le 1$, i.e. a partially entangled two-qubit state is more robust towards decoherence in comparison to a maximally entangled two-qubit state.

We now move forward to analyse the effect of weak measurements on the existence of nonlocal correlation in noisy conditions. For this, we assume that Charlie prepares a two-qubit entangled state $|\Psi\rangle = \alpha|00\rangle + \beta|11\rangle$, $(|\alpha|^2 + |\beta|^2 = 1)$ and performs weak measurements on both qubits before sending them through amplitude-damping channels. Similarly, after receiving the qubits, both Alice and Bob carry out the reversal of the weak measurement on their qubits. The weak measurement $\Lambda_i^{wk}$ and the reverse weak measurement $\Lambda_i^{\text{wkr}}$ operators performed at both ends can be given by

$$\Lambda_i^{wk} = \begin{pmatrix} 1 & 0 \\ 0 & \sqrt{1-\eta_i} \end{pmatrix} \text{ and } \Lambda_i^{\text{wkr}} = \begin{pmatrix} \sqrt{1-\eta_{ri}} & 0 \\ 0 & 1 \end{pmatrix} \tag{12}$$

where $\eta_i$ and $\eta_{ri}$ are the strengths of the weak measurement and the weak measurement reversal operations, respectively. The optimal weak measurement strength is defined by $\eta_{ri} = \eta_i + \gamma_i(1-\eta_i)$, where $i = 1, 2$ [21–23]. Assuming that the strength of the weak measurement reversal is optimal, the finally shared state between Alice and Bob evolves as

$$\rho_A^{wk} = \frac{1}{N_A} \begin{pmatrix} |\alpha|^2 + \gamma_1\gamma_2\eta_1'\eta_2'|\beta|^2 & 0 & 0 & \alpha^*\beta \\ 0 & \gamma_1\eta_1'|\beta|^2 & 0 & 0 \\ 0 & 0 & \gamma_2\eta_2'|\beta|^2 & 0 \\ \alpha\beta^* & 0 & 0 & |\beta|^2 \end{pmatrix} \tag{13}$$

where $N_A = 1 + \{\gamma_1\eta_1'(1+\gamma_2\eta_2') + \gamma_2\eta_2'\}|\beta|^2$ and $\eta_i' = (1-\eta_i)$ and $(i = 1, 2)$. For analytical optimisation of the Bell-CHSH operator, we first consider the first term representing the expectation value $\langle AC\rangle$ in (5), such that

$$\begin{aligned} \langle \sigma_1 \cdot \hat{a}\sigma_2 \cdot \hat{c}\rangle = \frac{1}{N_A}[&(\alpha^2 + (1+\gamma_1(\eta_1-1)) \\ &(1+\gamma_2(\eta_2-1))\beta^2)\cos\theta_a\cos\theta_c \\ &+ 2\alpha\beta\sin\theta_a\sin\theta_c\cos(\phi_a+\phi_c)] \end{aligned} \tag{14}$$

Similar to the way we evaluated the optimum value of the Bell-CHSH operator for $\rho_A^{\gamma}$, one can show that the optimum expectation value of the Bell-CHSH operator for $\rho_A^{wk}$ is

$$B(\rho_A^{wk})_{\text{opt}} = \frac{2}{N_A}\left[\begin{matrix}(\alpha^2 + (1+\gamma_1(\eta_1-1))(1+\gamma_2(\eta_2-1))\beta^2)^2 \\ +4\alpha^2\beta^2\end{matrix}\right]^{\frac{1}{2}} \tag{15}$$

For $\eta_i = 1$, the expression in (15) will be the same as for a pure state. This is possible as the state $\rho_A^{wk}$ becomes a pure state free from any decoherence for $\eta_i = 1$.

Figure 3 demonstrates the effect of the weak measurement strengths on the Bell-CHSH operator for a decoherence parameter value of $\gamma_1 = \gamma_2 = 0.5$ and $\alpha^2 = \frac{1}{\sqrt{2}}$. The state clearly violates the Bell inequality for $\gamma_i = 0.5$ when the values of $\eta_i$'s exceed a certain minimum, and the amount of violation increases with the increase in weak measurement strength. From Figure 2, one can conclude that if one starts with a maximally entangled two-qubit state, then, for $\gamma_i = 0.5$, the Bell-CHSH inequality is not violated. However, performing weak measurement and weak measurement reversal operations allows for the violation of the Bell-CHSH operator confirming the existence of nonlocal correlations in the finally shared entangled state. For simplicity, we consider a scenario where both channels have the same decoherence, i.e. $\gamma_1 = \gamma_2 = \gamma$, and both qubits are subjected to identical weak measurement strengths, i.e. $\eta_1 = \eta_2 = \eta$. In such a case, the optimal expectation value of the Bell-CHSH operator is

$$B(\rho_A^{\text{new}})_{\text{opt}} = \frac{2}{N_A'}[(\alpha^2 + (1+\gamma(\eta-1))^2\beta^2)^2 + 4\alpha^2\beta^2]^{\frac{1}{2}} \tag{16}$$

where $N_A' = (\alpha^2 + (1+\gamma(1-\eta))^2\beta^2)$. In order to compare the effects of the weak measurement vs. amplitude damping,

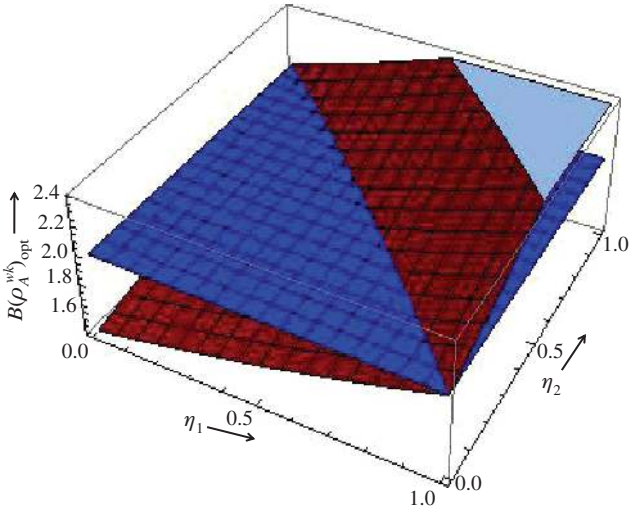


**Figure 3:** Estimation of $B(\rho_A^{wk})_{\text{opt}}$ with respect to weak measurement strengths $\eta_1$ and $\eta_2$ for a maximally entangled initial state, considering $\gamma = 0.5$.

in Figure 4, we show plots between the optimal expectation value of the Bell-CHSH operator and the weak measurement strength for different initial states considering that $\gamma = 0.6$. We consider a higher value of the noise parameter as in the absence of weak measurement, the Bell-CHSH inequality is not violated by all states. We again observe that a partially entangled initial state with a higher $\alpha$ is a better and robust resource in comparison to a maximally entangled initial state. Moreover, depending on the initial state used, the Bell-CHSH inequality is violated by the finally shared state only after a certain value of the weak measurement strength $\eta$. In general, the nonviolation regime increases with a decrease in the value of $\alpha$. For a given initial state, we further deduce a condition $((\alpha^2+(1+\gamma(\eta-1))^2\beta^2)^2+4\alpha^2\beta^2) \geq (\alpha^2+(1+\gamma(1-\eta))^2\beta^2)^2$ for the violation of the Bell-CHSH inequality by a finally shared state. For example, if $\gamma = 0.6$, then, for an initial state with $\alpha = \frac{1}{\sqrt{2}}$, the strength of the weak measurement required for the violation of the Bell-CHSH inequality is $0.5953 \leq \eta \leq 1$.

For a maximally entangled initial state, Figures 5 and 6 describe the effects of the noise parameter $\gamma$ for different values of the weak measurement strength $\eta$ and the effects of the weak measurement strength $\eta$ for the different values of the noise parameter $\gamma$. Clearly, the weak measurement and its reversal is a win-win situation for enhancing the correlations between the qubits. Similarly, Figures 7 and 8 illustrate the relation between the violation of the Bell-CHSH operator and the value of $\alpha$ for different values of the noise parameter $\gamma$ for $\eta = 0$ and the different values of the weak measurement strength for $\gamma = 0.6$, respectively.

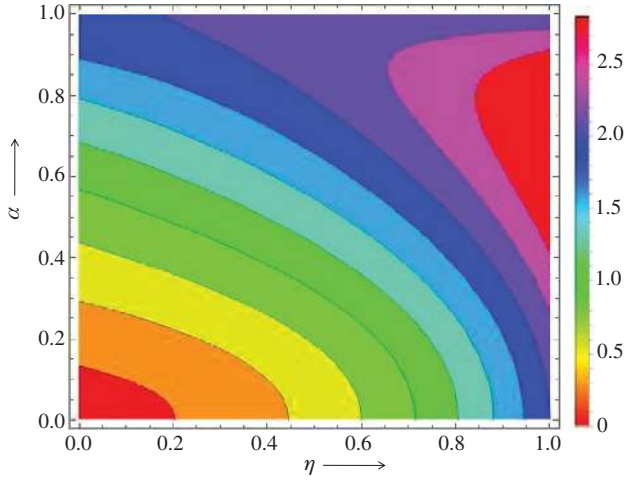


**Figure 4:** Effect of weak measurement strength $\eta$ on $B(\rho_A^{new})_{opt}$, for different two-qubit entangled states, considering the noise parameter $\gamma = 0.6$.

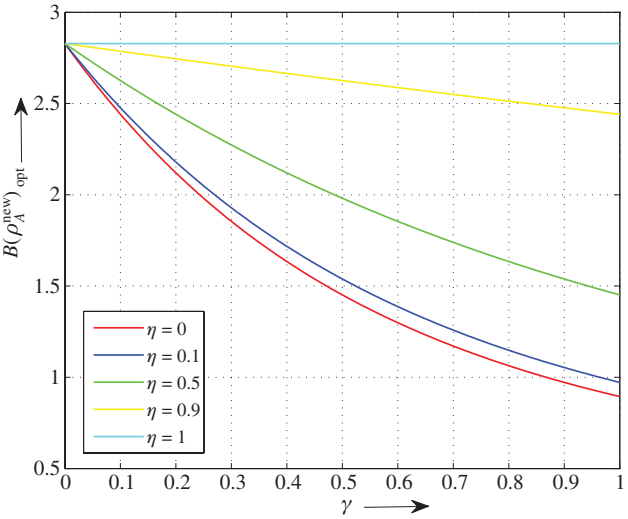


**Figure 5:** Effect of decoherence on $B(\rho_A^{new})_{opt}$ for a maximally entangled input state at different values of weak measurement strength $\eta$.

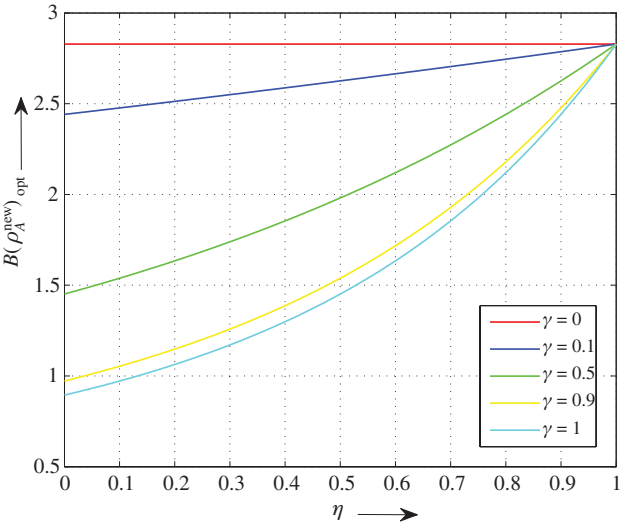


**Figure 6:** Comparison of the Bell inequality violation vs. weak measurement strength $\eta$ for a maximally entangled input state at different values of decoherence parameter.

## 2.2 Alternative Method to Estimate Violation of the Bell-CHSH Operator

Horodecki et al. [56] have shown a necessary and sufficient condition for the violation of the CHSH inequality by an arbitrary spin $-\frac{1}{2}$ state. According to Horodecki's theorem, the maximum possible violation of the CHSH inequality for any arbitrary 2-qubit state $\rho$ is given by

$$B_{max} = 2\sqrt{M(\rho)} \tag{17}$$

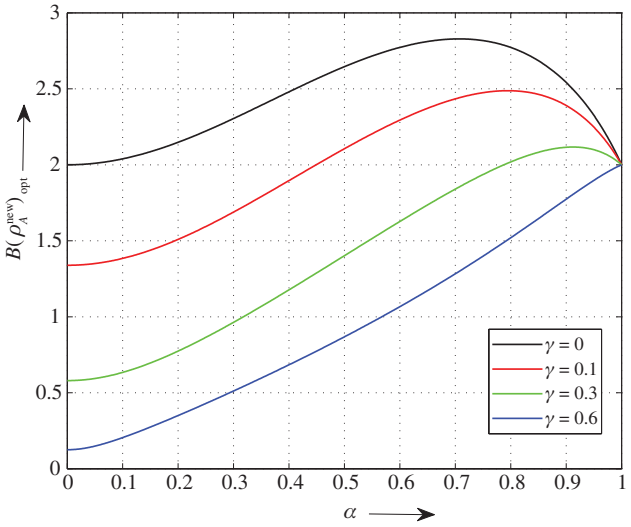


**Figure 7:** Comparison of $B(\rho_A^{new})_{opt}$ vs. state parameter $\alpha$ at different values of noise parameter $\gamma$, considering $\eta = 0$.

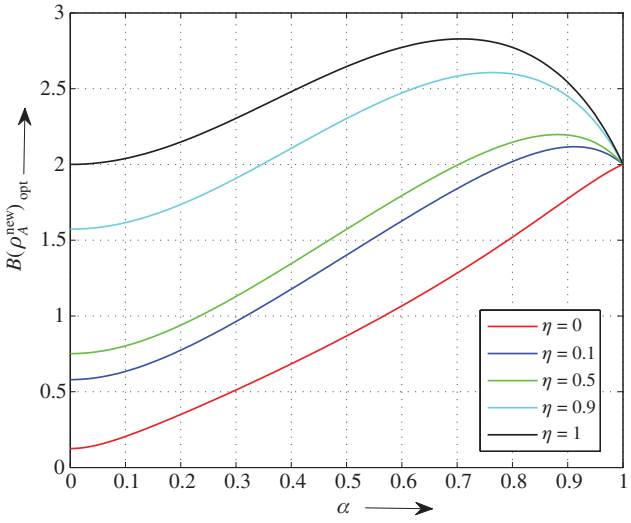


**Figure 8:** Comparison of $B(\rho_A^{new})_{opt}$ vs. state parameter $\alpha$ for different values of weak measurement strength considering $\gamma = 0.6$.

where $M(\rho) = \max_{i<j}(u_i + u_j)$, and $u_i$ $(i = 1, 2, 3)$ are the eigenvalues of $U = T^T T$. Here, $T^T$ denotes the transposition of T, and inequality (1) is violated by an arbitrary two-qubit state iff $M(\rho) > 1$. Therefore, we calculate $M(\rho_A^{wk})$ considering the identical noise parameters $\gamma_1 = \gamma_2 = \gamma$ and identical weak measurement strengths $\eta_1 = \eta_2 = \eta$, such that

$$M(\rho_A^{new}) = \frac{(\alpha^2 + (1+\gamma(\eta-1))^2\beta^2)^2 + 4\alpha^2\beta^2}{(\alpha^2 + (1+\gamma(1-\eta))^2\beta^2)^2} \tag{18}$$

and hence,

$$B(\rho_A^{new})_{opt} = \frac{2[(\alpha^2 + (1+\gamma(\eta-1))^2\beta^2)^2 + 4\alpha^2\beta^2]^{\frac{1}{2}}}{(\alpha^2 + (1+\gamma(1-\eta))^2)\beta^2)} \tag{19}$$

One can clearly see that (19) is the same as (16) obtained in this article analytically.

## 2.3 Phase-Damping Channel

In the case of a phase-damping channel, the Kraus operators can be represented as

$$E_0 = \begin{pmatrix} 1 & 0 \\ 0 & \sqrt{1-\gamma_i} \end{pmatrix}, E_1 = \begin{pmatrix} 0 & 0 \\ 0 & \sqrt{\gamma_i} \end{pmatrix} \tag{20}$$

where $\gamma$ represents the phase-damping noise parameter, and $i = 1, 2$ represents the qubit index. Again, for simplicity, we consider that both qubits comprising the initial input state are transmitted through an identical decoherence channel, i.e. $\gamma_1 = \gamma_2 = \gamma$. Similar to the case of the amplitude-damping channel, the input state shared between Alice and Bob now evolves as

$$\rho_P^{\gamma} = \begin{pmatrix} |\alpha|^2 & 0 & 0 & (1-\gamma)\alpha^*\beta \\ 0 & 0 & 0 & 0 \\ 0 & 0 & 0 & 0 \\ (1-\gamma)\alpha\beta^* & 0 & 0 & |\beta|^2 \end{pmatrix} \tag{21}$$

Therefore, using the Horodecki's theorem, the optimum expectation value of the Bell-CHSH operator is given as

$$B(\rho_P^{\gamma})_{opt} = 2\sqrt{1 + 4\alpha^2\beta^2(\gamma-1)^2} \tag{22}$$

Figure 9 describes the effect of decoherence on the correlations after both the qubits pass through

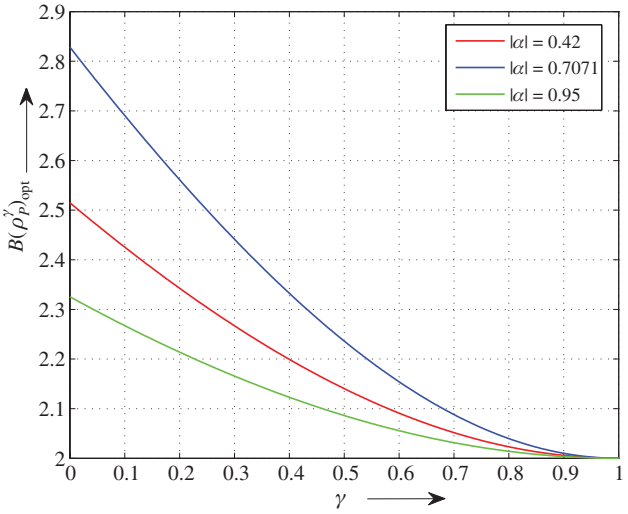


**Figure 9:** Effect of decoherence $\gamma$ on $B(\rho_P^{\gamma})_{opt}$ for different two-qubit entangled states.

phase-damping channels. Unlike the case of the amplitude-damping channel, where a nonmaximally entangled state seems to be more robust than a maximally entangled state for a particular range of decoherence parameter, here, the maximally entangled state is always robust in comparison to the nonmaximally entangled states. For a given two-qubit initial state, the finally shared state always violates the Bell inequality for the whole range of decoherence parameters.

In order to analyse the effect of the weak measurement and its reversal, we again assume that before sending the qubits through phase-damping channels, Charlie first performs weak measurements on both the qubits as given in (12). After receiving the qubits, Alice and Bob perform weak measurement reversal operations on their respective qubits. Therefore, the finally shared state between Alice and Bob evolves as

$$\rho_P^{wk} = \frac{1}{N_P}\begin{pmatrix} |\alpha|^2\eta_r'^2 & 0 & 0 & \alpha^*\beta\gamma'\eta'\eta_r' \\ 0 & 0 & 0 & 0 \\ 0 & 0 & 0 & 0 \\ \alpha\beta^*\gamma'\eta'\eta_r' & 0 & 0 & |\beta|^2\eta'^2 \end{pmatrix} \tag{23}$$

where $\eta' = (1-\eta)$, $\eta_r' = (1-\eta_r)$, $\gamma' = (1-\gamma)$, and $N_P = (|\alpha|^2 (1-\eta_r)^2 + |\beta|^2(1-\eta)^2)$. The optimised value of the Bell-CHSH operator for the state $\rho_P^{wk}$ can be calculated in a similar fashion as in the case of $\rho_P^{\gamma}$, and can be given as

$$B(\rho_P^{wk})_{\text{opt}} = \sqrt{1 + \frac{4\alpha^2\beta^2(1-\gamma)^2(1-\eta)^2(1-\eta_r)^2}{\alpha^2(1-\eta_r)^2 + \beta^2(1-\eta)^2}} \tag{24}$$

The optimal weak measurement reversal strength leading to maximum correlations between the qubits is evaluated to be $\eta_r = 1-(1-\eta)\frac{\beta}{\alpha}$. Hence, assuming the strength of the measurement reversal operation to be optimal, the expectation value of the Bell-CHSH operator is given as

$$B(\rho_P^{wk})_{\text{opt}} = 2\sqrt{1+(\gamma-1)^2} \tag{25}$$

Equation (25) interestingly shows that the maximum expectation value of the Bell-CHSH operator of a shared bipartite state is independent of the parameter $\alpha$ and weak measurement strength $\eta$. Moreover, $B(\rho_P^{wk})_{\text{opt}} \geq B(\rho_P^{\gamma})_{\text{opt}}$ provided $\alpha^2\beta^2 \leq \frac{1}{2}$, which is always true for a two-qubit entangled state. Hence, the application of weak measurement can, indeed, be useful in upgrading the nonlocal correlations against the phase-damping decoherence. For optimal reversing weak measurement strength, Figure 10 clearly indicates that the maximum expectation value of the Bell-CHSH operator for the finally shared does not depend on the initial input state and is always the same as for a maximally entangled initial state. The use of weak measurement and its reversal protocol, therefore, provides a flexibility to communication protocols such that one can choose to start with any initial two-qubit pure state. However, for non-optimal weak measurement reversal, i.e. assuming $\eta_r = 0.2$ and a given input state considering $\alpha = 0.42$, the effect of the weak measurement strengths on the maximum expectation value of the Bell-CHSH operator for different values of the noise parameter is depicted in Figure 11.

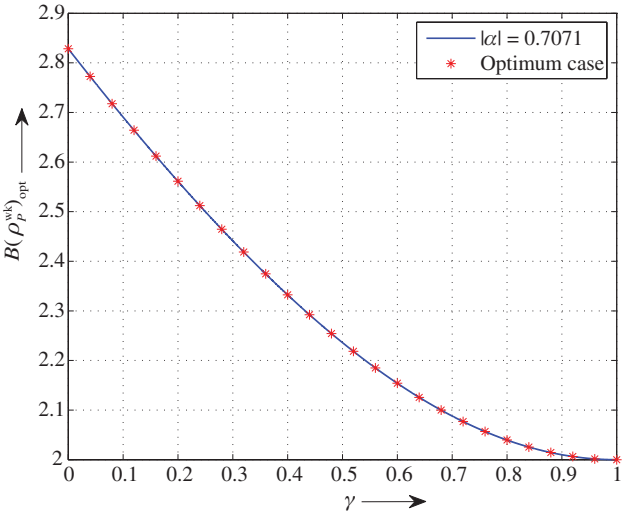


**Figure 10:** Effect of decoherence on $B(\rho_P^{wk})_{\text{opt}}$ for a maximally entangled state and any partially entangled input state under the application of weak measurement.

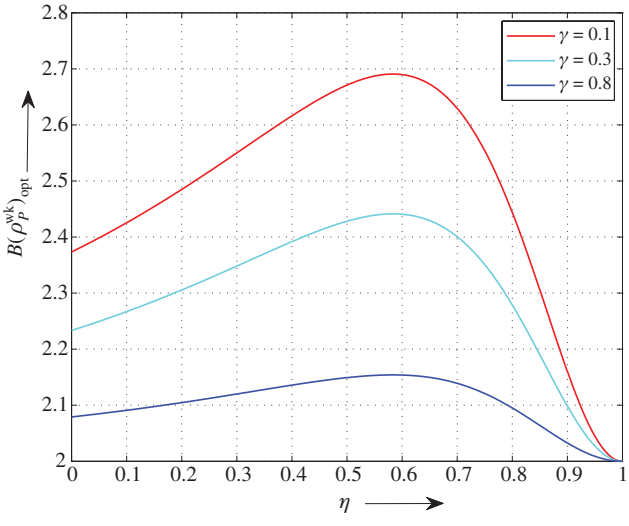


**Figure 11:** Effect of weak measurement on $B(\rho_P^{wk})_{\text{opt}}$ for non-optimal weak measurement reversal strength $\eta_r = 0.2$, for different values of decoherence parameter $\gamma$ considering $\alpha = 0.42$.

## 2.4 Depolarising Channel

Finally, we consider another important decoherence channel characterised by depolarising noise such that the single-qubit Kraus operators are described as

$$D_0 = \sqrt{1-\gamma}\begin{pmatrix}1 & 0\\ 0 & 1\end{pmatrix}, D_1 = \sqrt{\frac{\gamma}{3}}\begin{pmatrix}0 & 1\\ 1 & 0\end{pmatrix}$$
$$D_2 = \sqrt{\frac{\gamma}{3}}\begin{pmatrix}1 & 0\\ 0 & -1\end{pmatrix}, D_3 = \sqrt{\frac{\gamma}{3}}\begin{pmatrix}0 & -i\\ i & 0\end{pmatrix} \quad (26)$$

where $\gamma$ is a decoherence parameter. Here, we again consider the identical decoherence channel, i.e. $\gamma_1=\gamma_2=\gamma$. In this case, the initial state after passing through the depolarising channel can be given as

$$\rho_D^{\gamma} = \begin{pmatrix} f_{11} & 0 & 0 & f_{14}\\ 0 & f_{22} & 0 & 0\\ 0 & 0 & f_{33} & 0\\ f_{14}^{*} & 0 & 0 & f_{44}\end{pmatrix} \quad (27)$$

where

$$f_{11} = \frac{1}{9}(|\alpha|^2(3-2\gamma)^2 + 4|\beta|^2\gamma^2) \quad (28)$$

$$f_{14} = \frac{1}{9}\alpha^{*}\beta(3-4\gamma)^2 \quad (29)$$

$$f_{22} = f_{33} = \frac{2}{3}\gamma - \frac{4}{9}\gamma^2 \quad (30)$$

$$f_{44} = \frac{1}{9}(|\beta|^2(3-2\gamma)^2 + 4|\alpha|^2\gamma^2) \quad (31)$$

Thus, the optimum expectation value of $B(\rho_D^{\gamma})$ of the two-qubit state $\rho_D^{\gamma}$ shared between Alice and Bob is

$$B(\rho_D^{\gamma})_{\text{opt}} = \frac{2}{9}\sqrt{(1+4\alpha^2\beta^2)(3-4\gamma)^4} \quad (32)$$

Figure 12 demonstrates the effect of the noise parameter $\gamma$ on the expectation value of the Bell-CHSH operator for three different initial states, i.e. for $\alpha=\frac{1}{\sqrt{2}}$, $\alpha=0.95$ and $\alpha=0.42$. One can observe that the violation of the Bell-CHSH inequality decreases very fast even for small values of noise parameters.

We now consider to analyse the effect of the weak measurement and quantum measurement reversal on nonlocal correlations of the finally shared state.

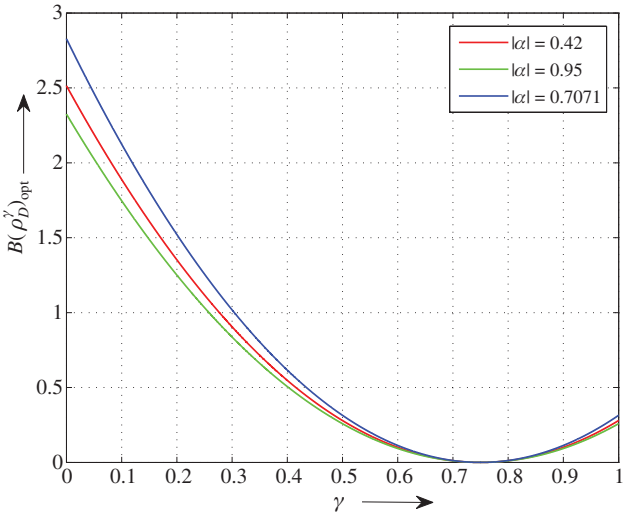


**Figure 12:** Effect of decoherence $\gamma$ on $B(\rho_D^{\gamma})_{\text{opt}}$ for different two-qubit entangled states.

For the depolarising channel, we replace $\sqrt{1-\eta}$ with $\mu$ and $\sqrt{1-\eta_r}$ with $\mu_r$ in (12) such that the expressions of the weak measurement and the weak measurement reversal operations are now given as $\Delta^{wk}=\begin{pmatrix}1 & 0\\ 0 & \mu\end{pmatrix}$ and $\Delta^{\text{wkr}}=\begin{pmatrix}\mu_r & 0\\ 0 & 1\end{pmatrix}$, respectively [57]. Similar to the previous cases, the finally shared state between Alice and Bob evolves as

$$\rho_D^{\gamma} = \frac{1}{N_D}\begin{pmatrix} g_{11} & 0 & 0 & g_{14}\\ 0 & g_{22} & 0 & 0\\ 0 & 0 & g_{33} & 0\\ g_{14}^{*} & 0 & 0 & g_{44}\end{pmatrix} \quad (33)$$

where

$$N_D = g_{11} + g_{22} + g_{33} + g_{44} \quad (34)$$

$$g_{11} = \mu_r^4(|\alpha|^2(3-2\gamma)^2 + 4|\beta|^2\gamma^2\mu^4) \quad (35)$$

$$g_{14} = \alpha^{*}\beta(3-4\gamma)^2\mu^2\mu_r^2 \quad (36)$$

$$g_{22} = g_{33} = 2\gamma(3-2\gamma)\mu_r^2(|\alpha|^2 + |\beta|^2\mu^4) \quad (37)$$

$$g_{44} = 4|\alpha|^2\gamma^2 + |\beta|^2(3-2\gamma)^2\mu^4 \quad (38)$$

The optimised value of the Bell-CHSH operator for the state $\rho_D^{wk}$ can be obtained in a similar fashion as discussed above, and can be given as

$$B(\rho_D^{wk})_{\text{opt}} = \frac{4}{N_D}[2\alpha^2\beta^2(3-4\gamma)^4\mu^4\mu_r^4]^{\frac{1}{2}} \quad (39)$$

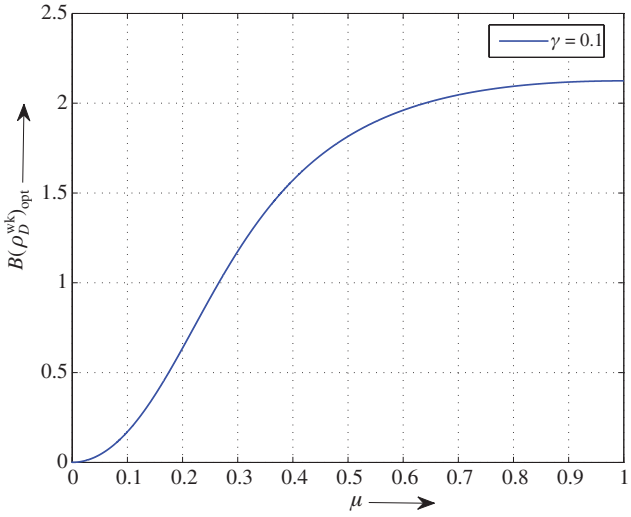


**Figure 13:** Effect of weak measurement on $B(\rho_D^{wk})_{opt}$ for a maximal entangled initial input state considering $\gamma = 0.1$.

The optimal reversing weak measurement strength, in the case of a depolarising channel, for maximising the amount of entanglement in the finally shared state is evaluated as

$$\mu_r = \left[\frac{(4|\alpha|^2\gamma^2 + |\beta|^2(3-2\gamma)^2\mu^4)}{(|\alpha|^2(3-2\gamma)^2 + 4|\beta|^2\gamma^2\mu^4)}\right]^{\frac{1}{4}} \tag{40}$$

Using (33), the maximum expectation value of the Bell-CHSH operator can be achieved for $\mu^2 = |\alpha|/|\beta|$, and can be expressed as

$$B(\rho_D^{wk})_{max} = \frac{2}{9}\sqrt{2(3-4\gamma)^4} \tag{41}$$

From (29) and (34), one can further deduce that $B(\rho_D^{wk})_{opt}$ is always greater than $B(\rho_D^{\gamma})_{opt}$. Furthermore, for the optimal weak measurement reversal strength and a maximally entangled initial input state, Figure 13 describes the effect of the weak measurement strength on the maximum expectation value of the Bell-CHSH operator considering that $\gamma = 0.1$.

# 3 A New Class of Mixed Entangled Two-Qubit States

Assuming that the input state is a two-qubit pure state, the finally shared state between Alice and Bob will either be a pure or a mixed state depending on the value of the weak measurement strength. Recently, Kim et al. [23] have shown that using the applications of the weak measurements and the amplitude-damping channel, the concurrence of the finally shared state is always non-zero, i.e. the finally shared state is always entangled. Ma et al. [58] have extended this study and proposed a set of states, which are entangled but do not violate the Bell-CHSH inequality after passing through the amplitude-damping channel. In this section, we characterise a new class of two-qubit mixed states using the weak measurements under the amplitude-damping noise. Interestingly, we found that the set of states proposed here are always entangled but do not violate the Bell-CHSH inequality for certain ranges of the amplitude-damping coefficient $\gamma$ and the weak measurement strength $\eta$. Further, our analysis shows that these states surprisingly outperform some of the mixed states already used as resources for quantum information processing.

For this purpose, we propose a class of two-qubit mixed states as

$$\varrho = \frac{1}{N}\left[\frac{1}{2}\gamma(1-\eta)\{\gamma(1-\eta)|00\rangle\langle 00| + |01\rangle\langle 01| + |10\rangle\langle 10|\} + |\Phi^+\rangle\langle\Phi^+|\right] \tag{42}$$

where $|\Phi^+\rangle = \frac{1}{\sqrt{2}}[|00\rangle + |11\rangle]$ and $N = \frac{1}{2}(2+\gamma(1-\eta)(2+\gamma(1-\eta)))$. In order to characterise the entanglement and correlations in this class, we use three different measures, i.e. concurrence, Bell inequality and geometric discord. For example, the concurrence of the proposed class is

$$C(\varrho) = \max\left\{0, \left(\frac{2-\gamma(1-\eta)}{2+\gamma(1-\eta)\left(2+\gamma(1-\eta)\right)}\right)\right\} \tag{43}$$

Moreover, the geometrical discord for an arbitrary spin $-\frac{1}{2}$ state is defined as

$$D_g(\rho) = \frac{1}{4}(||X||^2 + ||T||^2 - \lambda_{max}) \tag{44}$$

where $T$ is a matrix such that the elements of $T$ are $t_{ij} = Tr(\rho\sigma_i \otimes \sigma_j)$, $X$ is a vector in $R^3$ and $\lambda_{max}$ is the largest eigenvalue of matrix $K = XX^T + TT^T$. Here, we are only interested in the numerical estimation of the geometrical discord. As discussed above, the optimal expectation value of Bell-CHSH operator for the proposed class is

$$B(\varrho) = \frac{2[(1+(1+\gamma(\eta-1))^2)^2 + 4]^{\frac{1}{2}}}{(1+(1+\gamma(1-\eta))^2)} \tag{45}$$

Figures 14–16 demonstrate the effect of the weak measurement strength $\eta$ on concurrence, geometric discord, and Bell CHSH inequality for $\gamma = 0.6$, respectively. It is evident that the proposed class ($\varrho$) shows genuine

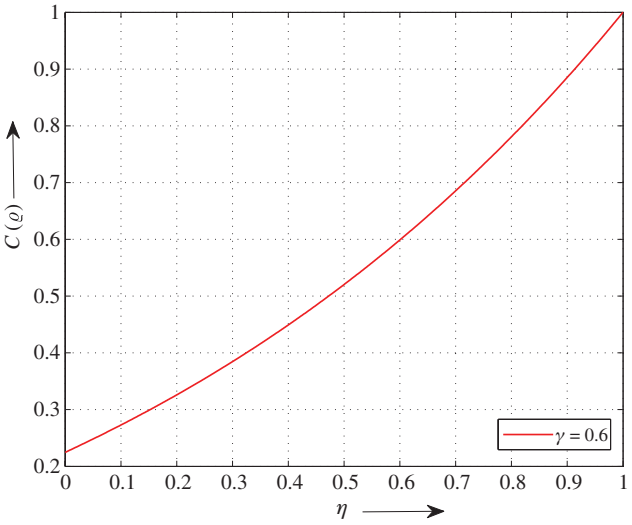


**Figure 14:** Concurrence of the proposed class $\varrho$ as a function of weak measurement strength, considering $\gamma = 0.6$.

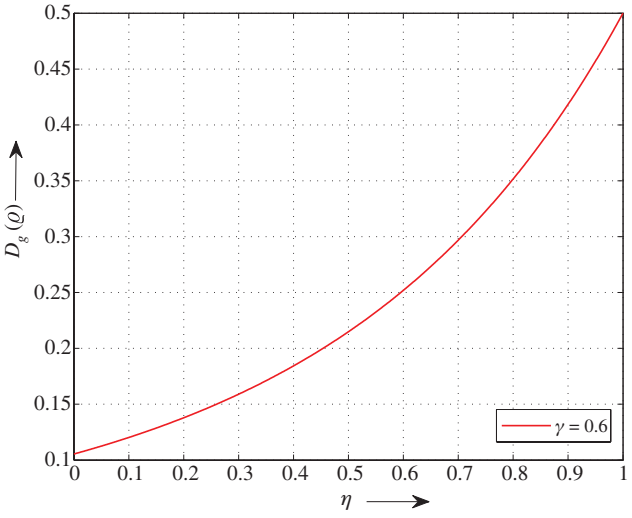


**Figure 15:** Geometrical discord of the proposed class $\varrho$ as a function of weak measurement strength, considering $\gamma = 0.6$.

entanglement and quantum correlations for all $\eta$ but violates the Bell-CHSH inequality for a range of weak measurement strengths, i.e. for $\max\left\{0, \left(1-\frac{0.2428}{\gamma}\right)\right\} < \eta \leq 1$.

# 4 Usefulness of the Proposed Two-Qubit Mixed State in Information Processing Tasks

In this section, we demonstrate the efficiency and usefulness of the proposed class of states in terms of quantum teleportation, dense coding and fully entangled fraction (FEF).

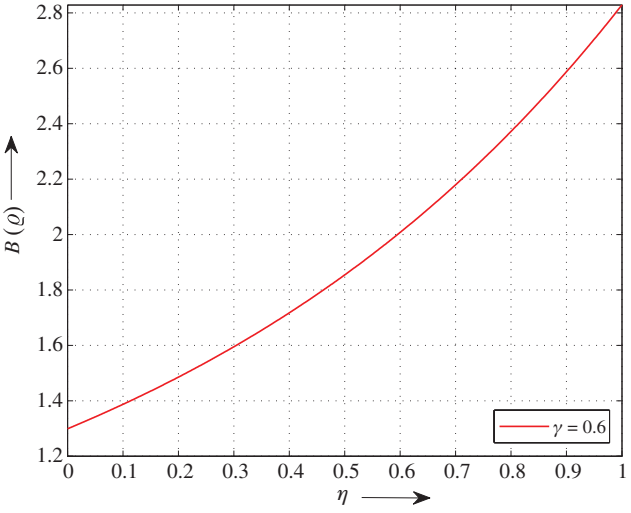


**Figure 16:** The optimal expectation value of the Bell-CHSH operator of the proposed state $\varrho$ as a function of weak measurement strength, considering $\gamma = 0.6$.

## 4.1 Quantum Teleportation

Quantum teleportation allows a sender to communicate quantum information using an entangled resource without sending the information through any medium. Horodecki et al. [24] described a measure of usefulness of the two-qubit mixed entangled states in terms of fidelity of quantum teleportation, namely,

$$F_{\max}(\rho) = \frac{1}{2}\left[1 + \frac{H(\rho)}{3}\right] \tag{46}$$

where $H(\rho) = \Sigma_{i=1}^{3}\sqrt{u_i}$ and $u_i$ $(i = 1, 2, 3)$ are the eigenvalues of the real symmetric matrix $U_\rho = T^T T$. They further deduced that a given state is useful as a resource for quantum teleportation iff $H(\rho) > 1$. In this subsection, we show that the class of states proposed in the previous section can always be used as a resource for quantum teleportation irrespective of the strength of decoherence and weak measurements. Surprisingly, when it comes to the fidelity of quantum teleportation, our states outperform many other mixed entangled two-qubit states. For this, we first calculate $H(\varrho)$ for $\varrho$, such that

$$H(\varrho) = 4\sqrt{\frac{1}{(1+(1+\gamma(1-\eta))^2)^2}} + \sqrt{\frac{(1+(1+\gamma(\eta-1))^2)^2}{(1+(1+\gamma(1-\eta))^2)^2}} \tag{47}$$

and hence,

$$F_{\max}(\varrho) = \frac{1}{2}\left[1+\frac{4}{3}\sqrt{\frac{1}{(1+(1+\gamma(\eta-1))^2)^2}}+\frac{1}{3}\sqrt{\frac{(1+(1+\gamma(\eta-1))^2)^2}{(1+(1+\gamma(1-\eta))^2)^2}}\right] \tag{48}$$

Figure 17 clearly indicates that the teleportation fidelity of the proposed state is always greater than 2/3. Therefore, this class of states are useful resources for quantum teleportation irrespective of the values of the noise parameter for the whole range of weak measurement parameter $\eta$.

Further, we compare the efficiency of our states as resources for teleportation fidelity with other existing bipartite mixed states. We first consider the two-qubit mixed Werner state [59], i.e.

$$\rho_W = (1-p)\frac{I_4}{4} + p|\psi^+\rangle\langle\psi^+| \tag{49}$$

where $p$ stands for the probability, $I$ stands for the identity matrix representing a white noise and $|\psi^+\rangle$ represents a maximally entangled Bell state, given by

$$|\psi^+\rangle = \frac{1}{\sqrt{2}}[|01\rangle+|10\rangle] \tag{50}$$

The teleportation fidelity of Werner state using (39) is

$$F_{\max}(\rho_W) = \frac{(p+1)}{2} \tag{51}$$

Similarly, for Horodecki's state [26], namely,

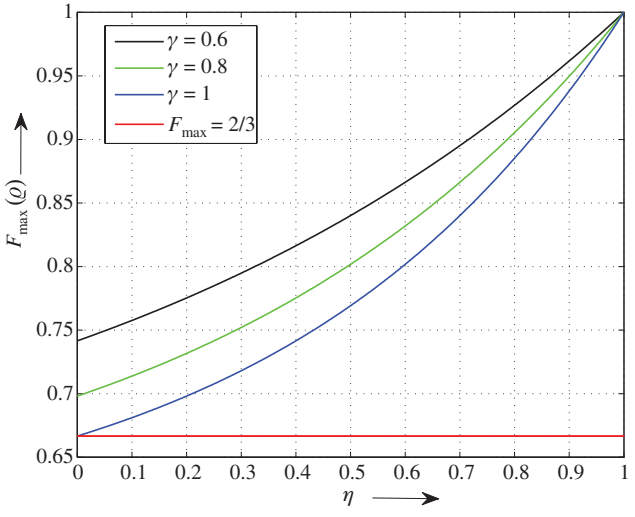


**Figure 17:** Teleportation fidelity of the proposed class of states $\varrho$ as a function of the weak measurement strength $\eta$ at different values of decoherence parameter $\gamma$.

$$\rho_h = (1-a)|00\rangle\langle 00| + a|\psi^+\rangle\langle\psi^+| \tag{52}$$

where $a$ stands for the state parameter, teleportation fidelity can be evaluated as

$$F_{\max}(\rho_h) = \begin{cases} \frac{2}{3} & a \le \frac{1}{2} \\ \frac{(2a+1)}{3} & a > \frac{1}{2} \end{cases} \tag{53}$$

We further consider another important class of two-qubit mixed states [60], termed as maximally entangled mixed states (MEMS), given by

$$\rho_{\text{MEMS}} = \begin{pmatrix} z(\delta) & 0 & 0 & \frac{\delta}{2} \\ 0 & 1-2z(\delta) & 0 & 0 \\ 0 & 0 & 0 & 0 \\ \frac{\delta}{2} & 0 & 0 & z(\delta) \end{pmatrix}$$

where

$$z(\delta) = \begin{cases} \frac{1}{3} & \delta < \frac{2}{3} \\ \frac{\delta}{2} & \delta \ge \frac{2}{3} \end{cases} \tag{54}$$

with $\delta$, a state parameter, denoting the concurrence of $\rho_{\text{MEMS}}$.

One can calculate the optimal teleportation fidelity for $\rho_{\text{MEMS}}$, such that

$$F_{\max}(\rho_{\text{MEMS}}) = \begin{cases} \frac{(3\delta+5)}{9} & \delta < \frac{2}{3} \\ \frac{(2\delta+1)}{3} & \delta \ge \frac{2}{3} \end{cases} \tag{55}$$

A more general class of MEMS was proposed by Wei et al. [61] as a mixture of maximally entangled Bell state $|\Phi_+\rangle$ and mixed diagonal state. Therefore, the general form of MEMS is given by

$$\rho^G_{\text{MEMS}} = \begin{pmatrix} q+\frac{\lambda}{2} & 0 & 0 & \frac{\lambda}{2} \\ 0 & s & 0 & 0 \\ 0 & 0 & t & 0 \\ \frac{\lambda}{2} & 0 & 0 & r+\frac{\lambda}{2} \end{pmatrix}$$

where $q, r, s, t$ and $\lambda$ are non-negative real state parameters such that $(q+r+\lambda+s+t)=1$. The teleportation fidelity for $\rho^G_{\text{MEMS}}$ is given by

$$F_{\max}(\rho^{G}_{\text{MEMS}}) = \frac{2}{3} + \frac{1}{3}(\lambda - s - t) \tag{56}$$

From (49), the optimal teleportation fidelity of $\rho^{G}_{\text{MEMS}}$ can be obtained by considering $s = 0$, $t = 0$ such that we get

$$F_{\max}(\rho^{G}_{\text{MEMS}}) = \frac{2}{3} + \frac{\lambda}{3} \tag{57}$$

Figure 18 compares the efficiency of the proposed state in this article with the two-qubit Werner state, Horodecki state, $\rho_{\text{MEMS}}$ and $\rho^{G}_{\text{MEMS}}$ for quantum teleportation. It clearly shows that the state proposed here is always a better resource in comparison to the Werner, Horodecki and $\rho_{\text{MEMS}}$ states. In the case of $\rho^{G}_{\text{MEMS}}$, our state proves to be a better resource for teleportation under weak decoherence; however, for strong decoherence, either our state or $\rho^{G}_{\text{MEMS}}$ can be considered as a preferred resource depending on the values of the state parameters. Moreover, for $s \neq 0$ or $t \neq 0$, the proposed state will always be a better resource for teleportation compared to $\rho^{G}_{\text{MEMS}}$.

## 4.2 Fully Entangled Fraction

Our analysis in the last subsection suggests that the proposed state is always a better resource in comparison to other established two-qubit mixed state for quantum teleportation protocol. In this subsection, we extend our analysis to the FEF $f_{\text{ent}}$, which is an entanglement witness and can be defined as

$$f_{\text{ent}}(\rho) = \max_{\phi} \langle \phi | \rho | \phi \rangle \tag{58}$$

where the maximum is taken over all maximally entangled two-qubit states $|\phi\rangle$ [25, 62]. Entanglement witnesses facilitates the experimental detection of entanglement and exist as a result of the Hahn-Banach theorem [26, 27, 63]. Moreover, FEF is considered as an emerging tool in describing many practical quantum information processing protocols [64–72]. For quantum teleportation, Horodecki et al. [25] have shown that a shared bipartite entangled state is useful for teleportation iff $f_{\text{ent}} > \frac{1}{2}$, where the relation between FEF and the optimal teleportation fidelity $F_{\max}$ is given by

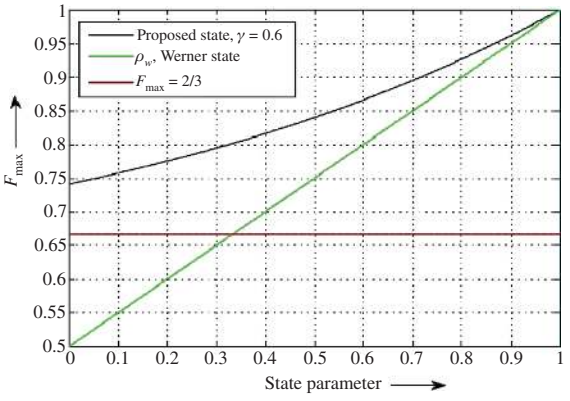


Comparison of the teleportation fidelity of proposed class of states and Werner state.

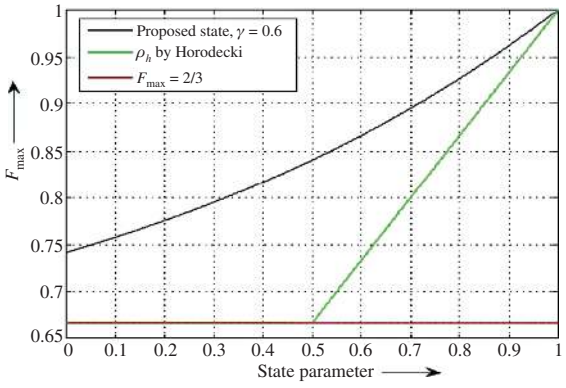


Comparison of the teleportation fidelity of proposed class of states and Horodecki's state.

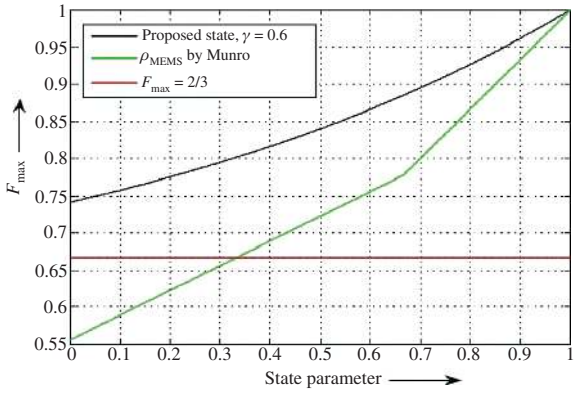


Comparison of the teleportation fidelity of proposed class of states and MEMS state proposed by Munro et al.

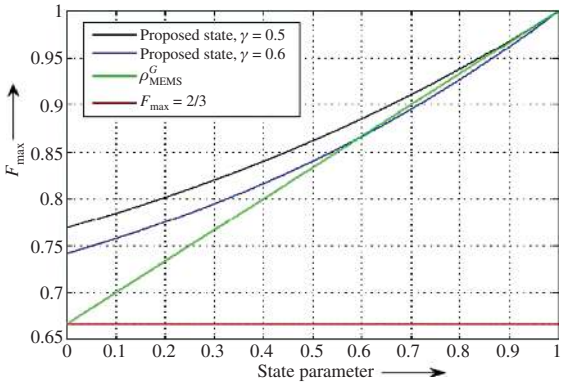


Comparison of the teleportation fidelity of proposed class of states and generalized MEMS state proposed by Wei et al.

**Figure 18:** Comparison of the usefulness of proposed class with other existing bipartite entangled mixed states.

$$F_{\max} = \frac{2f_{\text{ent}} + 1}{3} \tag{59}$$

As teleportation fidelity of the proposed class of states is always greater than 2/3, the FEF of the proposed class of states is always greater than 1/2. Figure 19 indicates the same by showing the effect of the weak measurement strength on the FEF of the proposed state at three different values of the amplitude-damping parameter.

We further consider three different witnesses to measure entanglement and correlations in the proposed class of states, namely, the modified or rescaled version of FEF [73], nonlinear entropic measure [74] and Horodecki's measure $M(\rho)$ [26]. The modified FEF detects a larger set of entangled states in comparison to the other two measures. For this, Bartkiewicz et al. proposed an efficient and realistic experimental procedure based on entanglement swapping to detect entanglement using the modified FEF defined as

$$F^W = \frac{1}{2}(Tr\sqrt{U} - 1) = 2f_{\text{ent}} - 1 \tag{60}$$

where $F^W < 0$ corresponds to separable states, and the maximum value of $F^W = 1$ corresponds to the maximally entangled states.

The form of the nonlinear entropic entanglement witness [74] is given by

$$E^W = \frac{1}{2}(TrU + |Tr\rho_a^2 - Tr\rho_b^2| - 1) \tag{61}$$

where the value of $E^W$ varies from 0 for separable states to 1 for the maximally entangled two-qubit states. In addition, for quantifying nonlocal correlations in two-qubit states, one may define Horodecki's measure $M(\rho)$ [26] as

$$M^W = TrU - \min[\text{eig}(U)] - 1 = M(\rho) - 1 \tag{62}$$

which is greater than 0 if a two-qubit state violates the Bell-CHSH inequality and attains the maximum value 1 for the maximally entangled state. $M(\rho)$ is directly related to the degree of Bell-CHSH inequality violation, such that $B'(\rho) = \sqrt{\max[0, M^W]}$ [75, 76].

Figure 20 shows that the proposed class of states are always entangled for the complete range of weak

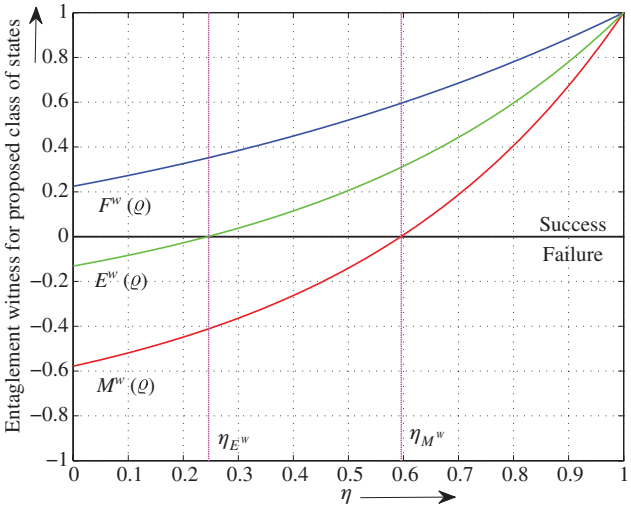


**Figure 20:** Estimating the entanglement of proposed class of states using the Bell nonlocality measure $M^W$, nonlinear entanglement witness $E^W$ and the rescaled FEF $F^W$ as a function of weak measurement strength $\eta$, considering $\gamma = 0.6$.

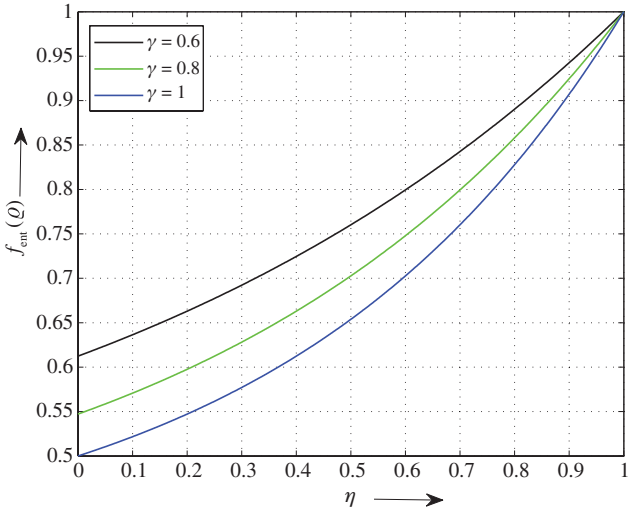


**Figure 19:** FEF as a function of weak measurement strength $\eta$ at different values of decoherence parameter $\gamma$.

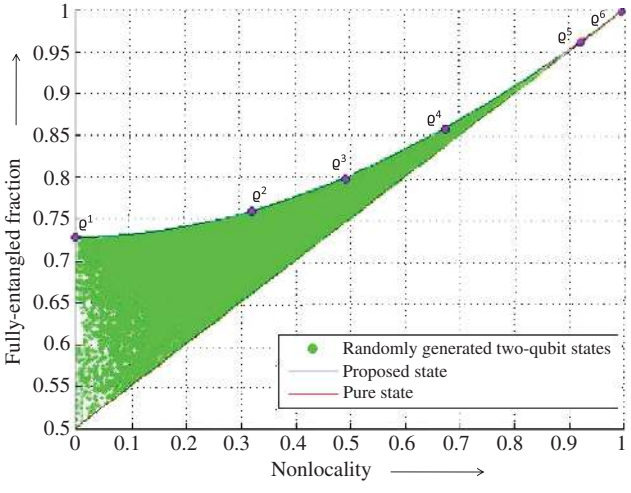


**Figure 21:** Estimation of FEF for a given nonlocality for proposed class of states, pure states and for randomly generated two-qubit states (green area) and the coordinates of points $\varrho^k$ (where $k = 1, \ldots, 6$).

**Table 1:** FEF $f_{ent}$ and nonlocality $B'$ measures of the proposed states $\varrho^k$ (for $k=1, \ldots, 6$) for different values of $\gamma$ and $\eta$.

| State | $\gamma$ | $\eta$ | $f_{ent}$ | $B'$ |
|---|---|---|---|---|
| $\varrho^1$ | 0.6 | 0.4126 | 0.7288 | 0.0000 |
| $\varrho^2$ | 0.6 | 0.4984 | 0.7596 | 0.3217 |
| $\varrho^3$ | 0.8 | 0.7000 | 0.7994 | 0.4922 |
| $\varrho^4$ | 0.4 | 0.6000 | 0.8581 | 0.6738 |
| $\varrho^5$ | 0.1 | 0.6000 | 0.9611 | 0.9199 |
| $\varrho^6$ | 0.6 | 0.9970 | 0.9982 | 0.9963 |

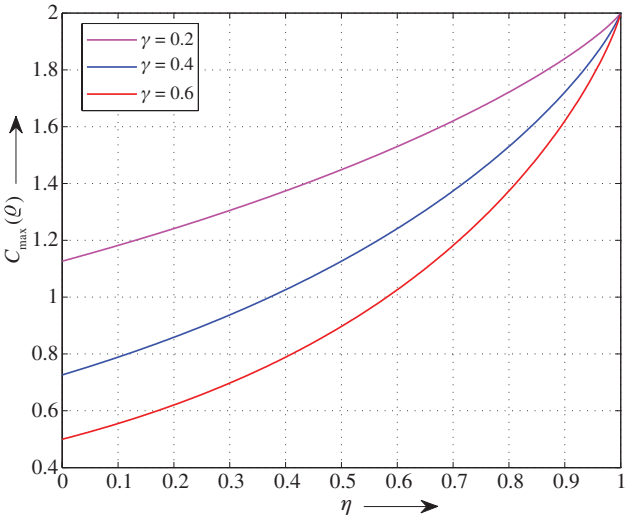


**Figure 22:** Channel capacity of superdense coding of the proposed class $\varrho$ as a function of the weak measurement strength $\eta$ at a different value of decoherence parameter $\gamma$.

measurement strength $\eta$ for $\gamma=0.6$, thereby, highlighting the importance of the proposed class of states for quantum information processing protocols. However, the linear entropic witness $E^W$ and Bell nonlocality measure $M^W$ can detect the entanglement and nonlocality in the proposed class of states for $\eta_{E^W} \geq \max\left\{0, \left(1-\frac{0.4534}{\gamma}\right)\right\}$, and $\eta_{M^W} \geq \max\left\{0, \left(1-\frac{0.2428}{\gamma}\right)\right\}$, respectively.

We further compare the FEF of the proposed class of states for a given degree of nonlocality $B'(\varrho)$ with the randomly generated two-qubit states [76].

For example, Figure 21 numerically estimates the FEF of the proposed class of states, pure states and $10^6$ randomly generated two-qubit states. It shows that the proposed class of states have higher FEF than the pure states and a large set of mixed two-qubit states for a given nonlocality. Here, we have only considered the states lying between our states and the pure states. In Table 1, we present characteristic points $\varrho^k$ (where $k=1, \ldots, 6$) for different values of $\eta$ and $\gamma$.

## 4.3 Dense Coding

Superdense coding is one of the simplest application of quantum information processing [1]. The usefulness of any shared entangled resource in dense coding is measured in terms of channel capacity, i.e. the maximum number of classical bits transmitted from a sender to a receiver using the shared resource [28] where the channel capacity using a bipartite entangled state $\rho^{AB}$ shared between Alice and Bob is given by

$$C_{\max} = \log_2 D_A + S(\rho^B) - S(\rho^{AB}) \tag{63}$$

where $D_A$ is the dimension of Alice's subsystem, $S(\rho^B)$ is the von-Neumann entropy of Bob's subsystem $\rho^B$ and $S(\rho^{AB})$ is the von-Neumann entropy of the entangled state $\rho^{AB}$.

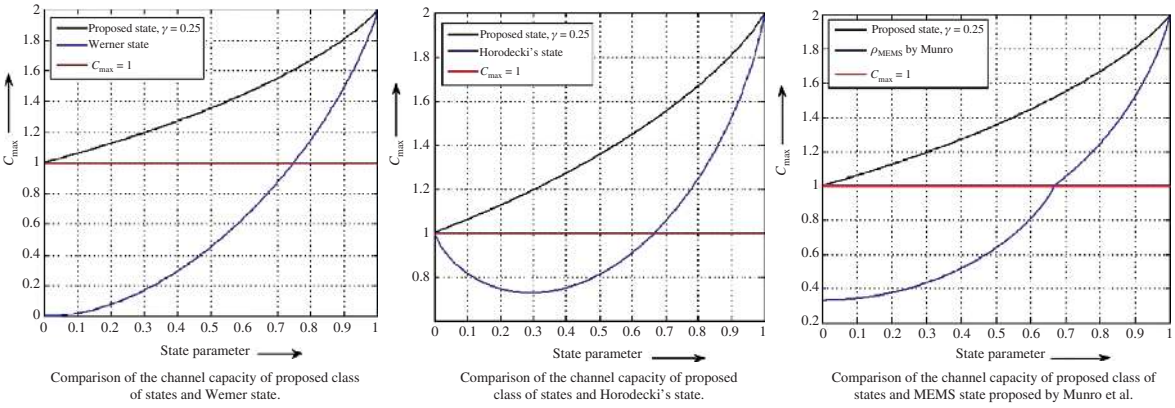


**Figure 23:** Comparison of the channel capacity of the proposed class with other bipartite entangled mixed states.

Figure 22 suggests that the channel capacity of the proposed class is always greater than 1 for weak decoherence and increases with an increase in the value of the weak measurement strength. However, for strong decoherence, the channel capacity only exceeds the classical channel capacity for large values of the weak measurement strength. Therefore, our states are useful resources for superdense coding even at high decoherence for a certain range of $\eta$. Furthermore, Figure 23 compares the efficiency of the proposed class with the Werner states, Horodecki states and $\rho_{\text{MEMS}}$ for superdense coding in terms of channel capacity. It clearly shows that our states are better resources for superdense coding in comparison to the Werner, Horodecki and $\rho_{\text{MEMS}}$ states.

## 5 Conclusion

In this article, we readdressed the issue of usefulness of two-qubit mixed states under noisy conditions. For this, we demonstrated the analytical relation between the Bell-CHSH inequality with noise parameters and the weak measurement strength parameters. The analysis allowed us to propose a new class of two-qubit mixed entangled states for quantum information processing protocols. The study presented here proved to be useful as our class of states is shown to be better resources in comparison to many other two-qubit mixed states proposed earlier for the similar communication protocols.

## References


[1] C. H. Bennett and S. Wiesner, Phys. Rev. Lett. **69**, 2881 (1992).
[2] C. H. Bennett, G. Brassard, C. Crépeau, R. Jozsa, A. Peres, et al., Phys. Rev. Lett. **70**, 1895 (1993).
[3] K. Bostrom and T. Felbinger, Phys. Rev. Lett. **89**, 187902 (2002).
[4] N. Gisin, G. Ribordy, W. Tittel and H. Zbinden, Rev. Mod. Phys. **74**, 145 (2002).
[5] M. Zukowski, A. Zeilinger, M. A. Horne and A. Eckert, Phys. Rev. Lett. **71**, 4287 (1993).
[6] A. Einstein, B. Podolsky and N. Rosen, Phys. Rev. **47**, 777 (1935).
[7] D. Bohm and Y. Aharanov, Phys. Rev. **108**, 1070 (1957).
[8] J. Batle, A. R. Plastino, M. Casas and A. Plastino, J. Phys. A **35**, 307 (2002).
[9] J. Batle and M. Casas, J. Phys. A **44**, 445304 (2011).
[10] J. Batle, C. H. Ooi, A. Farouk and S. Abdalla, Quant. Inf. Proc. **15**, 1553 (2016).
[11] J. Batle, M. Naseri, M. Ghoranneviss, A. Farouk, M. Alkhambashi, et al., Phys. Rev. A **95**, 032123 (2017).
[12] S. Bell, Physics **1**, 195 (1964).
[13] J. F. Clauser, M. A. Horne, A. Shimony and R. A. Holt, Phys. Rev. Lett. **23**, 880 (1969).
[14] E. Knill and R. Laflamme, Phys. Rev. Lett. **81**, 5672 (1998).
[15] S. Luo, Phys. Rev. A **77**, 042303 (2008).
[16] A. Dutta, A. Shaji and C. M. Caves, Phys. Rev. Lett. **100**, 050502 (2008).
[17] B. Dakic, V. Vedral and C. Brukner, Phys. Rev. Lett. **105**, 190502 (2010).
[18] G. F. Zhang, H. Fan, A. L. Ji and W. M. Liu, Eur. Phys. J. D **66**, 34 (2012).
[19] W. H. Zurek, Mod. Phys. Rev. **75**, 715 (2003).
[20] M. P. Almeida, F. de Melo, M. Hor-Meyll, A. Salles, S. P. Walborn, et al., Science **316**, 579 (2007).
[21] A. N. Korotkov and K. Keane, Phys. Rev. A **81**, 040103 (2010).
[22] J. C. Lee, Y.-C. Jeong, Y.-S. Kim and Y.-H. Kim, Opt. Express **19**, 16309 (2011).
[23] Y. S. Kim, M. C. Kuzyk, K. Han, H. Wang and G. Bahl, Nature Phys. **8**, 117 (2012).
[24] R. Horodecki, M. Horodecki and P. Horodecki, Phys. Lett. A **222**, (1996).
[25] M. Horodecki, P. Horodecki and R. Horodecki, Phys. Rev. A **60**, 1888 (1999).
[26] M. Horodecki, P. Horodecki and R. Horodecki, Phys. Lett. A **223**, 1 (1996).
[27] B. M. Terhal, Phys. Lett. A **271**, 319 (2000).
[28] G. Bowen, Phys. Rev. A **63**, 022302 (2001).
[29] C. H. Bennett, G. Brassard, S. Popescu, B. Schumacher, J. A. Smolin, et al., Phys. Rev. Lett. **76**, 722 (1996).
[30] C. H. Bennett, H. J. Bernstein, S. Popescu and B. Schumacher, Phys. Rev. A **53**, 2046 (1996).
[31] J. W. Pan, S. Gasparoni, R. Ursin, G. Weihs and A. Zeilinger, Nature **423**, 417, (2003).
[32] P. G. Kwiat, A. J. Berglund, J. B. Alterpeter and A. G. White, Science **290**, 498 (2000).
[33] D. A. Lidar, I. L. Chuang and K. B. Whaley, Phys. Rev. Lett. **81**, 2594 (1998).
[34] P. W. Shor, Phys. Rev. A **52**, R2493 (1995).
[35] A. R. Calderbank and P. W. Shor, Phys. Rev. A **54**, 1098 (1996).
[36] E. Knill and R. Laflamme, Phys. Rev. A **55**, 900 (1997).
[37] A. M. Steane, Phys. Rev. Lett. **77**, 793 (1996).
[38] P. Facchi, D. A. Lidar and S. Pascazio, Phys. Rev. A **69**, 032314 (2004).
[39] S. Maniscalco, F. Francica, R. L. Zaffino, N. L. Gullo and F. Plastina, Phys. Rev. Lett. **100**, 090503 (2008).
[40] A. N. Korotkov and A. N. Jordan, Phys. Rev. Lett. **97**, 166805 (2006).
[41] Y. S. Kim, Y. W. Cho, Y. S. Ra and Y. H. Kim, Opt. Express **17**, 11978 (2009).
[42] X. Xiao and Y. L. Li, Eur. Phys. J. D **67**, 204 (2013).
[43] Y. W. Cheong and S. W. Lee, Phys. Rev. Lett. **109**, 150402 (2012).
[44] Q. Sun, M. Al-Amri and M. Suhail Zubairy, Phys. Rev. A **80**, 033838 (2009).
[45] G. S. Paraoanu, Phys. Rev. Lett. **97**, 180406 (2006).
[46] B. Bellomo, R. Lo Franco, S. Maniscalco and G. Compagno, Phys. Rev. A **78**, 060302(R) (2008).
[47] J. T. Barreiro, M. Müller, P. Schindler, D. Nigg, T. Monz, et al., Nat. Phys. **6**, 943 (2010).
[48] R. Lo Franco, B. Bellomo, E. Andersson and G. Compagno, Phys. Rev. A **85**, 032318 (2012).

[49] N. Katz, M. Neeley, M. Ansmann, R. C. Bialczak, M. Hofheinz, et al., Phys. Rev. Lett. **101**, 200401 (2008).
[50] Q. Sun, M. Al-Amri, L. Davidovich and M. S. Zubairy, Phys. Rev. A **82**, 052323 (2010).
[51] G. S. Paraoanu, Phys. Rev. A **83**, 044101 (2011).
[52] X. Y. Xu, M. Neeley, M. Ansmann, R. C. Bialczak, M. Hofheinz, et al., Phys. Rev. Lett. **111**, 033604 (2013).
[53] N. Katz, M. Ansmann, R. C. Bialczak, E. Lucero, R. McDermott, et al., Science **312**, 1498 (2006).
[54] J. P. Groen, D. Ristè, L. Tornberg, J. Cramer, P. C. de Groot, et al. Phys. Rev. Lett. **111**, 090506 (2013).
[55] S. Popescu and D. Rohrlich, Phys. Lett. A **166**, 293 (1992).
[56] R. Horodecki, P. Horodecki and M. Horodecki Phys. Lett. A **200**, 340 (1995).
[57] J. He and L. Ye, Physica A **419**, 7 (2015).
[58] W. C. Ma, S. Xu, J. Shi and L. Ye, Phys. Lett. A **379**, 2802 (2015).
[59] R. F. Werner, Phys. Rev. A **40**, 4277 (1989).
[60] W. J. Munro, D. F. V. James, A. G. White and P. G. Kwiat, Phys. Rev. A **64**, 030302 (2001).
[61] T. C. Wei, K. Nemoto, P. M. Goldbart, P. G. Kwiat, W. J. Munro, et al., Phys. Rev. A **67**, 022110 (2003).
[62] C. H. Bennett, D. P. DiVincenzo, J. A. Smolin and W. K. Wootters, Phys. Rev. A **54**, 3824 (1996).
[63] R. B. Holmes, Geometric Functional Analysis and its Applications, Springer-Verlag, Berlin, 1975.
[64] S. Albeverio, S. M. Fei and W. L. Yang, Phys. Rev. A **66**, 012301 (2002).
[65] Z. W. Zhou and G. C. Guo, Phys. Rev. A **61**, 032108 (2000).
[66] G. Vidal, D. Jonathan and M. A. Nielsen, Phys. Rev. A **62**, 012304 (2000).
[67] M. J. Zhao, Z. G. Li, S. M. Fei and Z. X. Wang, J. Phys. A **43**, 275203 (2010).
[68] J. Grondalski, D. M. Etlinger and D. F. V. James, Phys. Lett. A **300**, 573 (2002).
[69] A. Kumar, S. Adhikari and P. Agrawal, Quant. Inf. Proc. **12**, 2475 (2013).
[70] S. K. Özdemir, K. Bartkiewicz, Y. X. Liu and A. Miranowicz, Phys. Rev. A **76**, 042325 (2007).
[71] M. Li, S. M. Fei and Z. X. Wang, Phys. Rev. A **78**, 032332 (2008).
[72] Z. G. Li, M. J. Zhao, S. M. Fei, H. Fan and W. M. Liu, Quantum Inf. Comp. **12**, 63 (2012).
[73] K. Bartkiewicz, K. Lemr, A. Černoch and A. Miranowicz, Phys. Rev. A **95**, 030102(R) (2017).
[74] F. A. Bovino, G. Castagnoli, A. Ekert, P. Horodecki, C. M. Alves, et al., Phys. Rev. Lett. **95**, 240407 (2005).
[75] A. Miranowicz, Phys. Lett. A **327**, 272 (2004).
[76] B. Horst, K. Bartkiewicz and A. Miranowicz, Phys. Rev. A **87**, 042108 (2013).